Performance of Spatial Diversity DCO-OFDM in a Weak Turbulence Underwater Visible Light Communication Channel

Jiang, H., Qiu, H., He, N., Popoola, W., Ahmad, Z. & Rajbhandari, S.

Performance of Spatial Diversity DCO-OFDM in a Weak Turbulence Underwater Visible Light Communication Channel

Hongyan Jiang, Hongbing Qiu, Ning He, Wasiu Popoola, *Senior Member, IEEE*, Zahir Ahmad, and Sujan Rajbhandari, *Senior Member, IEEE*

Abstract—The performance of underwater visible light communication (UVLC) system is severely affected by absorption, scattering and turbulence. In this paper, we study the performance of spectral efficient DC-biased optical orthogonal frequency division multiplexing (DCO-OFDM) in combination with the transceiver spatial diversity in turbulence channel. Based on the approximation of the weighted sum of lognormal random variables (RVs) that describe the oceanic turbulence condition, we derived a theoretical exact bit error rate (BER) for spatial diversity DCO-OFDM systems. The simulation results are compared with the analytical prediction, confirming the validity of the analysis. It is shown that spatial diversity can effectively reduce the turbulence induced channel fading. The obtained results can be useful for designing, predicting and evaluating the DCO-OFDM UVLC system in a weak oceanic turbulence condition.

Index Terms—underwater visible light communications (UVLC); spatial diversity; OFDM; turbulence mitigation

I. INTRODUCTION

AS the human activities in underwater environments for ocean exploration, environmental monitoring, scientific research, marine safety and other applications have increased, the demand for a high-speed, reliable and robust wireless communication is urgently required. There are a number of technologies currently being used for underwater communication, which has a number of limitations making them impractical for various applications. Radio Frequency (RF) is not suitable for underwater communication due to high absorption. Currently, acoustic communication is the dominant technique for underwater communication as it can achieve long-range data transmission. However, acoustic communication suffers from high latency and has limited bandwidth. Hence, the data rate is limited to a few kbps [1]. Recently, optical wireless communication (OWC) has attracted considerable attention due to the promise of license-free operation and high data rate. The low absorption in the blue-green optical spectrum and recent advances in light-emitting-diodes (LEDs) and laser diodes (LDs) technologies have enabled high-speed underwater visible light communication (UVLC) with low cost, small size and low power consumption [2]. UVLC is regarded as an effective complementary technology to conventional acoustic communication, providing an efficient and robust communication system between surface vehicles, underwater devices/divers and seafloor infrastructure [3]. Despite all these advantages, enabling reliable UVLC is very challenging as the UVLC channel is very dynamic and complex due to absorption, scattering, misalignment, turbulence and physical obstruction [4]. These factors cause high power loss, and random fading of the received optical signals. These adverse impairments not only limit the widespread usage of UVLC systems for longer ranges but also degrade the performance in short-range communications. Hence, it is essential to have a good understanding of the underwater channel; thereby adopt effective and efficient modulation scheme, coding and diversity techniques at the transmitter and receiver to mitigate the degrading effects.

Considerable research has been carried out to characterize the UVLC channel. Monte Carlo approach is a popular tool to simulate the channel. It uses statistical methods to obtain channel characteristics by tracking and recording the propagation of numerous photons through the medium [5], [6]. Gabriel *et al.* utilized the Monte Carlo approach and quantified time dispersion of optical signal for different water types [7]. A closed-form expression of the impulse response for a UVLC link is presented by using double-Gamma function to fit the

Hongyan Jiang and Hongbing Qiu are with the School of Information and Communication, Guilin University of Electronic Technology, Guilin 541004, China (e-mail: jhy8499@163.com, qiuhb@guet.edu.cn)

Ning He is with the School of Information and Communication, Guilin University of Electronic Technology, and also with Guangxi Key Laboratory of Wireless Wideband communication and Signal Processing, Guilin 541004, China (e-mail: eicnhe@guet.edu.cn)

Wasiu Popoola is with the School of Engineering, Institute for Digital Communications, University of Edinburgh, UK (e-mail: w.popoola@ed.ac.uk)

Zahir Ahmad and Sujan Rajbhandari is with the School of Computing, Electronics and Mathematics, Coventry University, UK (e-mail: ab7175@coventry.ac.uk and ac1378@coventry.ac.uk)

Corresponding author: Sujan Rajbhandari (e-mail: ac1378@coventry.ac.uk)

Monte Carlo simulation results [8]. To take multiple scattering into account, a weighted double-exponential model for a path loss is proposed in [9], [10] by fitting the UVLC simulation data obtained from the Monte Carlo method. F. Miramirkhani *et al* carried out a channel modelling and characterization study taking into account the presence of human and man-made objects to investigate the effects of shadowing and blockage [10]. Many of these studies focus on the effect of absorption and scattering on the channel, ignoring the turbulence induced fading which significantly impairs the performance [11]. Recently, many valuable studies have been performed to characterize the fading effects by multiplying the fading-free impulse response with a fading coefficient modelled as a lognormal random variable (RV) for weak oceanic turbulence [4], [11], [12].

Due to its simplicity and cost-effectiveness, UVLC uses intensity-modulation and direct-detection (IM/DD) with a simple modulation scheme such as on-off keying (OOK). However, the performance of the intensity based OOK modulation with a fixed threshold detection severely degrades even in weak turbulence [13]. The optimal performance can be obtained by considering adaptive thresholds, which require channel state information (CSI). However, due to a random fluctuation of the channel state, the adaptive threshold approach is practically very challenging. In order to overcome the limitations of OOK scheme, subcarrier intensity modulation (SIM) schemes such as subcarrier phase shift keying (SC-PSK) and subcarrier quadrature amplitude modulation (SC-QAM) have been proposed in optical communication systems [13]–[15]. In the SIM scheme, several independent SC streams are combined into intensity modulated optical signal which results in higher system throughput and flexibility in signal multiplexing [14]. Orthogonal frequency-division multiplexing (OFDM) is a special SC scheme with an orthogonal spacing of subcarrier. OFDM is widely utilized in the VLC system because of its high spectral efficiency, resilience to ISI and frequency-selective fading [16]–[18]. Though OFDM outperforms a number of modulation schemes in a band-limited channel, its performance is also impacted by the turbulence induced fading even in weak turbulence [18].

In order to mitigate the effect of oceanic turbulence on UVLC, several approaches have been studied such as adaptive optics [19], coding [20], relay-assisted network [21] and spatial diversity at the transmitter or/and receiver; also known as multiple-input-multiple-output (MIMO) system [4], [22]–[24]. Among them, spatial diversity is considered to be one of the most effective solutions. Spatial diversity can mitigate not only turbulence-induced fading but also effectively decrease the possibility of temporary blockage due to an obstruction (e.g., fish). Meanwhile, it also reduces the required power per source which helps to maintain the safe transmitting power density [22].

Though MIMO-OFDM has potential to provide a high data rate as well as mitigate the turbulence effect, to the best of the authors' knowledge, there is no prior work to evaluate the effectiveness of MIMO-UVLC with OFDM for the oceanic turbulence channel. Hence, in this work, we study the performance of DC-biased OFDM (DCO-OFDM) for UVLC in a weak turbulence channel. Applying the approximation to the weighted sum of lognormal RVs, we derived an analytical exact bit error rate (BER) for MIMO-OFDM with various spatial diversity orders in the presence of weak turbulence. Furthermore, the analytical results for different turbulence strength are verified using Monte-Carlo based simulation of DCO-OFDM with various diversity orders and DC-bias levels. DC-bias levels are optimized to avoid significant clipping noise due to low clipping level and waste of optical power due to a very high clipping level. Furthermore, the diversity gains for various diversity orders under different turbulence strength are also established.

The remainder of the paper is organized as follows. In Section II, the system and channel models are described in detail. In Section III, the BER performance analysis of the UVLC QAM-DCO-OFDM-MIMO systems is derived for the weak turbulence modelled by a lognormal distribution. In Section IV, the numerical results of channel characteristics and BER performance are presented. The paper concludes with a summary given in Section V.

II. MIMO-UVLC SYSTEM

A. System model

The block diagram of the proposed diversity MIMO-OFDM scheme is shown in Fig. 1 with *M* transmitters and *N* receivers. We have adopted the optical OFDM due to its spectral efficiency and resilience to ISI resulting from multipath propagation due to multiple scattering, particularly in harbor water. As described in various literatures, the traditional OFDM cannot be applied to IM/DD VLC (or OWC in general) due to the requirement of real and unipolar signal in IM/DD optical systems. Hence, various modified OFDMs have been proposed [25], [26]. In this work, we have adopted the DCO-OFDM as it outperforms other optical OFDM for UVLC [27]. In order to generate DCO-OFDM, we followed the standard practice of mapping input bits stream to *L*-QAM constellation (where $\log_2(L) > 0$ is an integer) followed by serial-to-parallel (S/P) conversion [28]. Then, to ensure real signal at the output of inverse fast Fourier transform (IFFT), the input symbol X_m to IFFT maintains a Hermitian symmetry, i.e. the subcarriers of the *L*-QAM OFDM symbol must satisfy:

$$X_m = X^*_{N_{fft}-m} , \quad 0 < m < \frac{N_{fft}}{2},$$
$$X_0 = X_{N_{fft}/2} = 0, \tag{1}$$

where * is the complex conjugate operation and N_{fft} is the fast Fourier transform (FFT) size.

In this work, we assume a short distance line-of-sight (LOS) link in coastal water. Due to a short delay spread and longer OFDM symbol duration, the effect of ISI is negligible. Furthermore, the focus of the study is to evaluate the performance of OFDM in turbulence UVLC channel and hence we only consider scattering-induced path loss and turbulence but ignore the ISI.

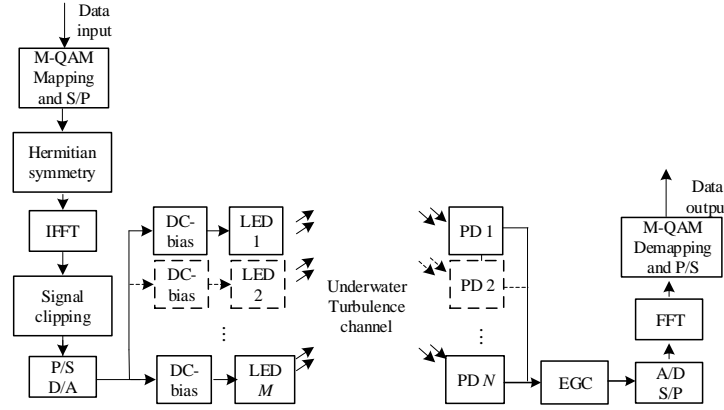The resulting signal after the IFFT operation is then clipped

Fig. 1. The block diagram of MIMO DCO-OFDM scheme for UVLC.

to the upper and lower levels to limit the dynamic range of DCO-OFDM signals. The clipping level affects the performance of DCO-OFDM. In this work, the optimization of the clipping level is not considered as this has been carried out in a number of studies [29], [30]. The clipped signal is converted to an analog signal by a digital-to-analog (D/A) converter, followed by addition of a suitable DC-bias to ensure a positive signal. The DC-bias I_{DC} is given as [25]:

$$I_{DC} = g\sqrt{E_s} , \qquad (2)$$

where g is the normalized bias and E_s is the energy per symbol. The signal is pre-clipped at $\pm I_{DC}$ to ensure positive signal after addition of DC-bias.

In this work, the repetition coding (RC) technique in which transmitters simultaneously emit the same signal is adopted as RC outperforms orthogonal space-time block codes for VLC [31]. The optical signal through an underwater oceanic channel experiences turbulence modelled as lognormal distribution (detail of the optical channel is provided in the following section) before being collected at the receiver. The received optical signal is firstly converted into an electrical signal and then combined using equal gain combining (EGC). Though the maximum ratio combining (MRC) is the optimal combining scheme, it requires the channel state estimation, which is challenging in a dynamic environment. Hence, the EGC is selected due to its simplicity.

In order to make a fair comparison between the system with and without diversity, the total transmitted optical power and receiver aperture are kept the same. Hence, the optical transmission power for each transmitter is P_s/M and receiver area for each receiver is D/N. For simplicity, D is normalized to 1 in the analysis in the following section. The MIMO channel includes path loss and turbulence $[\alpha_{mn}h_{mn}]_{m,n=1}^{M,N}$, where α_{mn} and h_{mn} represent the fading coefficient and channel path loss (or DC gain) from the mth transmitter to the nth receiver, respectively. Using RC and EGC, the received instantaneous electrical signal can be expressed as [14]:

$$y(t) = \frac{\eta k P_s}{MN} x(t) \sum_{m=1}^{M} \sum_{n=1}^{N} \alpha_{mn}h_{mn} + n(t) , \qquad (3)$$

where η denotes the photodiode (PD) responsivity, k is the

modulation index, $x(t)$ represents the OFDM signal, $|kx(t)| \leq 1$ and $n(t)$ is the additive white Gaussian noise (AWGN) signal.

The rest of processing is the same as the conventional OFDM receiver: FFT operation, followed by signal decoding. We use maximum likelihood detection (MLD) for signal detection i.e. the constellation vector $\hat{\mathbf{s}}$ is decided by the minimum Euclidean distance between the actually received signal vector $\mathbf{y}$ and all potential received signals as given by [31]:

$$\hat{\mathbf{s}} = \arg\max_{\mathbf{s}} P_y(\mathbf{y}|\mathbf{s}, \mathbf{H}) = \arg\min_{\mathbf{s}} ||\mathbf{y} - \mathbf{Hs}||_F^2 , \qquad (4)$$

where $\mathbf{H}$ is the channel matrix, $\mathbf{s}$ denotes all possible transmitted signal vectors, P_y is the probability of $\mathbf{y}$ conditioned on $\mathbf{s}$ & $\mathbf{H}$ and $||.||_F$ stands for the Frobenius norm.

B. Attenuation and Fading Statistics of UVLC Channel

The optical beam propagating through water has photons interacting with water molecules and other particles. The interaction induces energy conversion from optical to thermal or chemical, resulting in path loss. If the particle size is comparable to the wavelength and the refractive index varies, then photons change the transmission direction known as scattering. The scattering results in received photon loss due to the likelihood of photons deviating from the receiver aperture [24]. The phenomenon of absorption and scattering can be characterized by absorption coefficient $a(\lambda)$ and scattering coefficient $b(\lambda)$, where λ is the optical wavelength. Total effects of absorption and scattering on the energy loss are considered as attenuation characterised by extinction coefficient $c(\lambda) = a(\lambda) + b(\lambda)$. Hence, the received irradiance I after the transmission of distance d is calculated using the Beer-Lambert law given by:

$$I = I_0 e^{-c(\lambda)d} , \qquad (5)$$

where I_0 is the transmitted optical power.

Beer Lambert's law severely underestimates the received power especially in the scattering dominant regime as some of the scattered photons are still captured by the receiver [8]–[10]. So, it is more precise to use Monte-Carlo ray-tracing simulation to determine actual channel characteristics. In [8], the channel impulse response (CIR) is modelled by a double-Gamma function shown as follows:

$$h(t) = C_1 \Delta t e^{-C_2 \Delta t} + C_3 \Delta t e^{-C_4 \Delta t}, \qquad (6)$$

$$(t \geq t_0),$$

where C_1, C_2, C_3 and C_4 are the four parameters to be solved by the least mean square (LMS) fitting algorithm and $\Delta t = t - t_0$, where $t_0 = d/v$ is the propagation time i.e. the ratio of transmission distance d over light speed v in water. .Using CIR, the path loss and the root mean square (RMS) delay spread can be calculate, which provide reference to energy loss and maximum data rate, respectively [10],[15].To approximate the path loss $H(d)$ accurately, a weighted function of two exponentials is proposed as [9], [10]:

$$H(d) = a_1 e^{-a_2 d} + a_3 e^{-a_4 d}, \qquad (7)$$

where the weighted parameters a_1, a_2, a_3 and a_4 are similarly calculated by fitting to the Monte-Carlo simulation data.

Furthermore, fluctuations in temperature and salinity in the underwater cause a random variation in the refractive index causing optical turbulence. The turbulence results in optical signal fading. Lognormal distribution is widely used to model weak turbulence for both diffusive LED-based and collimated laser-based UWOC links [4], [22]–[24], [27]. The numerical and experimental studies in [32] have revealed that lognormal can aptly match the histogram of the acquired data in many of underwater channel conditions, although there are some specific scenarios where lognormal failed to model the fading. Moreover, the weighted sum of lognormal RVs is more easily approximated than other statistical distributions so that it is helpful to use probability density function (PDF) of fading model to directly evaluate the BER performance of EGC spatial diversity systems without the aid of moment generating function (MGF) and characteristic function (CHF). Therefore, we employ the lognormal fading model for weak oceanic turbulence in this paper, as given by [24]:

$$f(\alpha) = \frac{1}{2\alpha\sqrt{2\pi\sigma_\rho^2}} \exp\left(-\frac{(\ln(\alpha) - 2\mu_\rho)^2}{8\sigma_\rho^2}\right), \qquad (8)$$

where α is the turbulence-induced fading coefficient, expressed as $\alpha \sim \text{lognormal}(2\mu_\rho, 4\sigma_\rho^2)$, μ_ρ and σ_ρ^2 denote the mean and variance of the normal-distributed fading log-amplitude and $\rho = \frac{1}{2}\ln(\alpha) \sim \Omega(\rho, \mu_\rho, \sigma_\rho^2)$ is known as the fading log-amplitude. To ensure that no energy loss or gain during the turbulence-induced fading process, the fading amplitude is normalized, i.e. $\text{E}[\alpha] = 1$, leading to $\mu_\rho = -\sigma_\rho^2$, where $\text{E}[.]$ is the expectation operation. Usually, the scintillation index σ_I^2 is used to quantify the turbulence strength, which is defined as [24]:

$$\sigma_I^2 = \frac{\text{E}[I^2] - \text{E}^2[I]}{\text{E}^2[I]} = \frac{\text{E}[\alpha^2] - \text{E}^2[\alpha]}{\text{E}^2[\alpha]}. \qquad (9)$$

The relation between the scintillation index and log-amplitude variance can be described as:

$$\sigma_I^2 = \exp\left(4\sigma_\rho^2\right) - 1. \qquad (10)$$

In order to take into account turbulence effects, the channel impulse response is multiplied by a multiplicative fading coefficient $\alpha = \exp(2\rho)$.

III. BIT ERROR RATE ANALYSIS FOR EGC

From (3), the electrical signal-to-noise ratio (SNR) γ_{EGC} of ECG can be derived as [14]:

$$\gamma_{\text{EGC}} = \left(\frac{\eta k P_s}{MN\sigma}\right)^2 \text{E}[x^2(t)] \left(\sum_{m=1}^{M}\sum_{n=1}^{N} \alpha_{mn} h_{mn}\right)^2, \qquad (11)$$

where σ^2 is the AWGN variance.

For the transmitter-receiver diversity, we can simplify

$$\sum_{m=1}^{M}\sum_{n=1}^{N} \alpha_{mn} h_{mn} = \sum_{i=1}^{MN} \alpha_i h_i. \qquad (12)$$

Furthermore, we can use another lognormal variable to approximate the weighted sum of lognormal random variables [15][33] . So, we have

$$\sum_{i=1}^{MN} \alpha_i h_i = \alpha_{sum} = \text{e}^z, \qquad (13)$$

where α_{sum} is the weighted sum of log-normal distributed turbulence coefficients and z is the corresponding normal-distributed variable. Assuming all branches experience normalized independent identical distributed (i.i.d) lognormal fading, we can obtain the variance and mean of z as [33].

$$\sigma_z^2 = \ln\left[\frac{\sum_{i=1}^{MN}(e^{4\sigma_\rho^2}-1)h_i^2}{\left(\sum_{i=1}^{MN} h_i\right)^2} + 1\right],$$

and $\qquad (14)$

$$\mu_z = \ln\left[\sum_{i=1}^{MN} h_i\right] - \frac{\sigma_z^2}{2},$$

Substituting (12) and (13) into (11), we obtain:

$$\gamma_{EGC} = \bar{\gamma}\text{e}^{2z}, \qquad (15)$$

where $\bar{\gamma} = \left(\frac{\eta k P_s}{MN\sigma}\right)^2 \text{E}[x^2(t)]$ represents the average electrical SNR. The expression in (15) provides SNR for ECG diversity. Furthermore, the analytical expression for the BER performance of L-QAM O-OFDM can be approximated as follows [29], [30]:

$$p_e = \frac{4(\sqrt{L}-1)}{\sqrt{L}\log_2(L)} Q\left(\sqrt{\frac{3}{L-1}\gamma_{eff}}\right), \qquad (16)$$

where $Q(.)$ is the Gaussian-Q function, γ_{eff} is the effective electrical SNR per received symbol. When the DC-bias is large enough to avoid any clipping distortion, we have [30]:

$$\gamma_{eff} = \frac{1}{1+g^2}\gamma_{EGC}. \qquad (17)$$

In the turbulent channel, the average BER can be obtained by integrating BER expression over the fading coefficient. From (15), (16) and (17), the BER p_e is given by (18). So, by the approximation of the weighted sum of lognormal RVs an MN-dimensional integration is reduced to a one-dimensional integration, thereby we can deduce an exact BER for the spatial

diversity *L*-QAM O-OFDM system over weak oceanic turbulence.

IV. NUMERICAL RESULTS

In this section, we report numerical results obtained for the channel impulse response and BER performance of 4-QAM DCO-OFDM UVLC in the presence of weak turbulence. We employed Monte-Carlo Ray tracing method to simulate fading-free impulse response (FFIR) and path loss (PL). The simulation parameters are summarized in Table I.

TABLE I
SIMULATION PARAMETERS

Parameters		Value
Transmitter	Wavelength	532 nm
	Full beam divergence angle	10°
	No. of Transmitter	1, 2 and 4
	Transmitter separation	30 cm
Channel	Refractive index of Water, *n*	1.331
	Link distance	12 m
	Absorption coefficient	0.179 m^{-1} coastal water
	Scattering coefficient	0.219 m^{-1}
Receiver	Aperture diameter	20 cm
	Half angle FOV	90°
	No. of receiver	1,2 and 4
	Receiver separation	30 cm
	Photon weight threshold	10^{-4}

In order to verify the validity of the simulation results, we first simulated the optical path loss and FFIR using Monte Carlo Ray tracing approach and compared with the theoretical fitting functions in (7) and (6), respectively. Fig. 2 shows the path loss coefficient as a function of the link distance and FFIR of the optical link at a link distance of 12 m. Note that in Fig.2 (b), the start time of impulse response is shifted from t_0 to zero. The path loss coefficient as a function of distance fits well with a double-exponential function with an R-square of 0.9999. Similarly, the FFIR demonstrates a good match with a double-Gamma function fitting with the R-square value of 0.9979. These results confirmed the validity of Monte Carlo Ray tracing method. Moreover, the FFIR shown in Fig.2 (b) has an RMS delay spread of ~5.4 ps and hence the maximum symbol rate that can be supported without ISI is up to 18.5 Gbps. The bandwidth of the state-of-the-art LEDs is less than 1 GHz, which is significantly lower than the channel bandwidth, we did not consider ISI in the simulation as well as the BER analysis outlined in section above.

With this verification, we then calculated the FFIR and channel gain h_{mn} between the mth transmitter and n^{th} receiver for a diversity system with various orders. The channel matrixes for different diversity orders are given in Table II in terms of channel gain, where the diversity order is equal to the product of *M* transmitters and *N* receivers.

The focus of the study is to evaluate the performance of DCO-OFDM in the presence of turbulence while the

optimization of DC, i.e. clipping level, is not considered. However, in order to avoid the effect of clipping level on the BER performance, we first simulated the BER performance of single-channel in an AWGN channel with various normalized DC-levels. Fig. 3 displays the BER performance of 4-QAM DCO-OFDM for various DC-bias levels. The figure also shows the theoretical BER prediction using (16). Note that the SNR expression includes power due to the DC-bias level and modulating signal. As can be seen from the figure, the theoretical prediction and simulation results match closely for the large DC-bias level of $g \geq 3$ that avoids significant clipping distortion. There is a small deviation between the theoretical and simulated results for $g = 2$. However, at $g = 1$, the simulation results show that there is a BER floor of 10^{-3}. This is due to high clipping noise. The clipping noise is not included in the theoretical prediction and hence there is a difference in the theoretical and simulated BER for $g = 1$ & 2. Furthermore, the figure clearly demonstrates that increasing DC-bias level reduces the electrical power efficiency. Hence, $g = 3$ is selected in the rest of the study as this offers the best electrical power efficiency without any clipping noise.
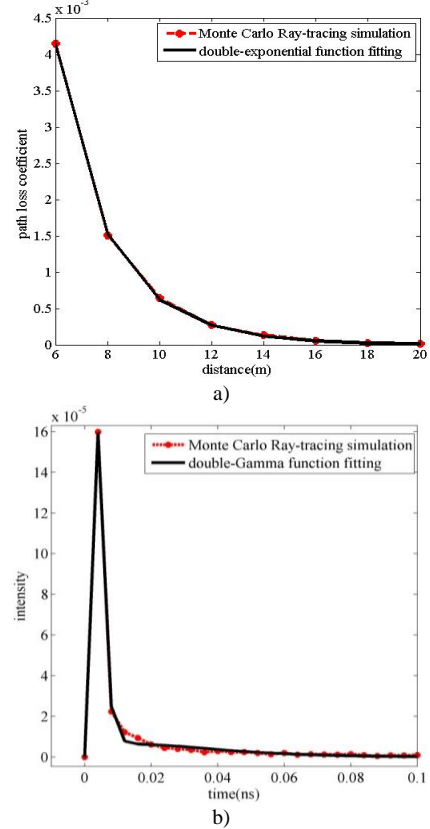

a)

b)

Fig.2. a) The path loss coefficient as a function of link distance in coastal water and b) the FFIR for a UVLC link with a distance of 12 m in the coastal water.

$$p_e = \int f(z)\, p_e(z)\, \mathrm{d}z = \int_{-\infty}^{\infty} \Omega(z, \mu_z, \sigma_z^2) \frac{4(\sqrt{L}-1)}{\sqrt{L}\log_2(L)} Q\left(e^z \sqrt{\frac{3\bar{\gamma}}{(L-1)(1+g^2)}}\right) \mathrm{d}z \qquad (18)$$

TABLE II
CHANNEL MATRIXES FOR DIFFERENT DIVERSITY ORDERS.

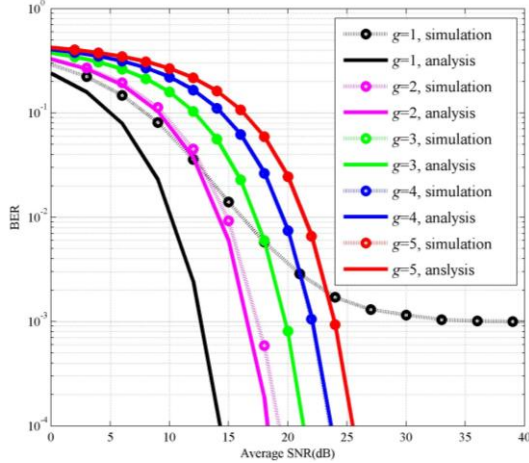| Diversity order ($M\times N$)	Channel matrix in terms of path loss
1×1	0.274×10^{-3}
1×2	$10^{-3}\times(0.140\ 0.140)$
2×2	$10^{-3}\times\begin{pmatrix}0.270 & 0.113\\0.113 & 0.270\end{pmatrix}$
2×4	$10^{-3}\times\begin{pmatrix}0.142 & 0.088 & 0.101 & 0.128\\0.088 & 0.142 & 0.128 & 0.101\end{pmatrix}$
4×4	$10^{-3}\times\begin{pmatrix}0.2830 & 0.1060 & 0.0890 & 0.1070\\0.1060 & 0.2830 & 0.0970 & 0.0930\\0.0890 & 0.0970 & 0.2830 & 0.0950\\0.1070 & 0.0930 & 0.0950 & 0.2830\end{pmatrix}$

Fig.3. The simulation and theoretical BER of 4-QAM DCO-OFDM in an AWGN channel without turbulence and with different DC-bias levels.

Using the parameters in Table II, we evaluate the BER performance of 4-QAM DCO-OFDM with various spatial diversity orders for a turbulence channel. A pseudorandom binary sequence (PRBS) of 2^{18} was generated and converted into an OFDM signal using the block diagram in Fig. 1. The UVLC turbulent channels are slow fading, i.e. the fading coefficient remains constant over millions of consecutive bits for the transmission rate on the order of Gbps [32]. Hence, we assumed the fading coefficient is constant over an OFDM symbol duration and changes with OFDM symbols. At the receiver, EGC was used, followed by standard OFDM decoding. Finally, the transmitted binary sequence is compared with the received sequence to calculate the BER. Fig. 4 shows the comparison of the theoretical and simulated BER for 4-QAM DCO-OFDM for a turbulence channel with $\sigma_I^2 = 0.7$. The simulated BERs match closely to the analytical BERs calculated by (18) for various diversity orders with identical or non-identical path loss, verifying the theoretical and simulation study.
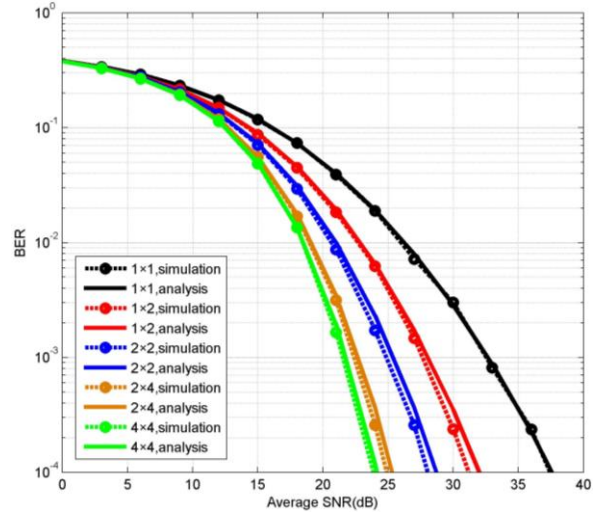

Fig.4. The theoretical lower bound (LB) and simulation BER performance 4-QAM DCO-OFDM in a weak oceanic turbulence channel with g =3 and $\sigma_I^2 = 0.7$ with different spatial diversity orders.

Fig. 5 shows the simulated BER performance of 4-QAM DCO-OFDM with spatial diversity orders of 1×1, 2×2 and 4×4 for a turbulence channel with $\sigma_I^2 = 0.1$ and 0.9. As a benchmark, the BER of a single channel in AWGN channel without turbulence is also given. Fig.5 demonstrates a clear advantage of diversity schemes in the presence of turbulence, especially for the strong turbulence. The diversity order of 2×2 and 4×4 outperforms the BER performance of the single channel. It is also obvious that as the turbulence strength increases, the BER performance of single-channel worsens. By comparison, turbulence strength has less influence on BER performance with a large diversity order. At $\sigma_I^2 = 0.1$, the BER performance for diversity order of 2×2 and 4×4 is very close but better than that of 1×1. However, at $\sigma_I^2 = 0.9$, diversity order of 4×4 offers improved BER performance in comparison to 2×2 and 1×1 with an SNR difference of 4.5 dB and 15.6 dB, respectively at a BER of 10^{-4}.
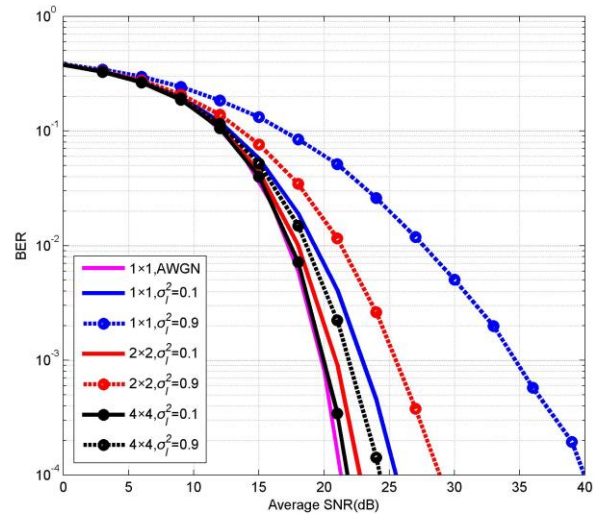

Fig. 5. The simulation BER performance of spatial diversity 4-QAM DCO-OFDM in oceanic turbulence channel with g = 3, and $\sigma_I^2 = 0.1$ & 0.9.

Furthermore, EGC diversity gain for various diversity orders in the oceanic turbulence channel with different scintillation indexes is summarized in Fig.6. Note that the diversity gain is the difference in SNR (dB) required to achieve a BER of 10^{-4} for the systems with and without diversity. It is noted that for weak turbulence e.g. $\sigma_I^2 = 0.1$, diversity order of 4 (i.e. a system with 2×2) is adequate to compensate for the turbulence effect as higher order does not provide further gain. However, as the turbulence strength increases, diversity gain also increases with increasing diversity orders. For example, diversity gain of 3.6 dB, 7.5 dB, 11.1 dB and 14.1 dB is obtained for diversity order of 8 with $\sigma_I^2 = 0.1, 0.3, 0.6 \; \& \; 0.9$, respectively. This clearly indicated that a larger diversity order is required to combat strong turbulence. Furthermore, error correction coding and equalization may be used in conjunction with diversity to further improve the performance.

V. CONCLUSION

In this paper, the BER performance of a spatial diversity UVLC system in weak oceanic turbulence channel was investigated based on M-QAM DCO-OFDM modulation with EGC. We derived a theoretical exact BER for M-QAM DCO-OFDM systems in the presence of weak turbulence assuming a lognormal distribution. We employed the Monte Carlo Ray tracing method to simulate the path loss and impulse response for various diversity orders. The BER of various diversity order was simulated and compared with the analysis. It is concluded that the higher diversity order is effective in mitigating the turbulence effect and diversity gain increases with the turbulence strength. For example, a diversity gain of 3.8 dB, and 15.6 dB was obtained using the diversity order of 16 with $\sigma_I^2 = 0.1 \; \& \; 0.9$, respectively. The obtained results can be useful for designing, predicting and evaluating the MIMO DCO-OFDM UVLC system in the weak oceanic turbulence condition.
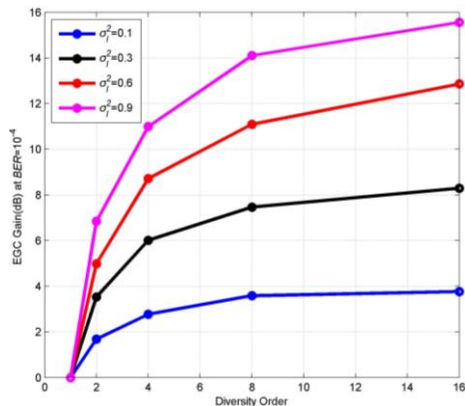

Fig.6. EGC diversity gain in a lognormal oceanic turbulence channel against the diversity order at BER $= 10^{-4}$ for 4-QAM DCO-OFDM with $g = 3$.

REFERENCE

[1] S. Arnon, "Underwater optical wireless communication network," *Opt. Eng.*, vol. 49, no. 1, pp. 1–6, 2010.

[2] S. Rajbhandari *et al.*, "A review of gallium nitride LEDs for multi-gigabit-per-second visible light data communications," *Semicond. Sci. Technol.*, vol. 32, no. 2, 2017.

[3] H. Kaushal and G. Kaddoum, "Underwater optical wireless communication," *IEEE Access*, vol. 4, pp. 1518–1547, 2016.

[4] M. V. Jamali, P. Nabavi, and J. A. Salehi, "MIMO underwater visible light communications: Comprehensive channel study, performance analysis, and multiple-symbol detection," *IEEE Trans. Veh. Technol.*, vol. 67, no. 9, pp. 8223–8237, 2018.

[5] C. D. Mobley *et al.*, "Comparison of numerical models for computing underwater light fields," *Appl. Opt.*, vol. 32, no. 36, p. 7484, Dec. 1993.

[6] Z. Ghassemlooy, S. Arnon, M. Uysal, Z. Xu, and J. Cheng, "Emerging Optical Wireless Communications-Advances and Challenges," *IEEE J. Sel. Areas Commun.*, vol. 33, no. 9, pp. 1738–1749, 2015.

[7] C. Gabriel, M.-A. Khalighi, S. Bourennane, P. Léon, and V. Rigaud, "Monte-Carlo-Based Channel Characterization for Underwater Optical Communication Systems," *J. Opt. Commun. Netw.*, vol. 5, no. 1, p. 1, Jan. 2013.

[8] S. Tang, Y. Dong, and X. Zhang, "Impulse response modeling for underwater wireless optical communication links," *IEEE Trans. Commun.*, vol. 62, no. 1, pp. 226–234, 2014.

[9] C. Wang, H. Y. Yu, and Y. J. Zhu, "A long distance underwater visible light communication system with single photon avalanche diode," *IEEE Photonics J.*, vol. 8, no. 5, pp. 1–11, 2016.

[10] F. Miramirkhani and M. Uysal, "Visible Light Communication Channel Modeling for Underwater Environments With Blocking and Shadowing," *IEEE Access*, vol. 6, pp. 1082–1090, 2018.

[11] C. T. Geldard, J. Thompson, E. Leitgeb, and W. O. Popoola, "Optical Wireless Underwater Channel Modelling in the Presence of Turbulence," in *2018 IEEE British and Irish Conference on Optics and Photonics (BICOP)*, 2018, pp. 1–4.

[12] S. Tang, X. Zhang, and Y. Dong, "Temporal statistics of irradiance in moving turbulent ocean," *Ocean. 2013 MTS/IEEE Bergen Challenges North. Dimens.*, pp. 0–3, 2013.

[13] W. O. Popoola and Z. Ghassemlooy, "BPSK subcarrier intensity modulated free-space optical communications in atmospheric turbulence," *J. Light. Technol.*, vol. 27, no. 8, pp. 967–973, 2009.

[14] H. D. Trung, B. T. Vu, and A. T. Pham, "Performance of free-space optical MIMO systems using SC-QAM over atmospheric turbulence channels," *IEEE Int. Conf. Commun.*, pp. 3846–3850, 2013.

[15] Z. Ghassemlooy, W. O. Popoola, and S. Rajbhandari, *Optical wireless communications – System and channel modelling with Matlab*, 1st ed. CRC Press, 2012.

[16] X. Song, Z. Zhao, Y. Wei, and M. Wang, "Research and performance analysis on multi-point light-emitting diodes-array intra-vehicle visible light communication systems with DC-biased optical–orthogonal frequency-division multiplexing," *Int. J. Distrib. Sens. Networks*, vol. 13, no. 9, 2017.

[17] M. Sharma, D. Chadha, and V. Chandra, "Capacity evaluation of MIMO-OFDM Free Space Optical communication system," *2013 Annu. IEEE India Conf. INDICON 2013*, pp. 1–4, 2013.

[18] A. Bekkali, C. Ben Naila, K. Kazaura, K. Wakamori, and M. Matsumoto, "Transmission analysis of OFDM-based wireless services over turbulent radio-on-FSO links modeled by gamma - Gamma distribution," *IEEE Photonics J.*, vol. 2, no. 3, pp. 510–520, 2010.

[19] I. Toselli and S. Gladysz, "Adaptive optics correction of scintillation for oceanic turbulence-affected laser beams," in *Environmental Effects on Light Propagation and Adaptive Systems*, 2018, p. 7.

[20] I. B. Djordjevic, B. Vasic, and M. A. Neifeld, "LDPC coded OFDM over the atmospheric turbulence channel," *Opt. Express*, vol. 15, no. 10, p. 6336, 2007.

[21] M. V. Jamali, F. Akhoundi, and J. A. Salehi, "Performance Characterization of Relay-Assisted Wireless Optical CDMA Networks in Turbulent Underwater Channel," *IEEE Trans. Wirel. Commun.*, vol. 15, no. 6, pp. 4104–4116, 2016.

[22] M. V. Jamali, J. A. Salehi, and F. Akhoundi, "Performance studies of underwater wireless optical communication systems with spatial diversity: MIMO Scheme," *IEEE Trans. Commun.*, vol. 65, no. 3, pp. 1176–1192, 2017.

[23] W. Liu, Z. Xu, and L. Yang, "SIMO detection schemes for underwater optical wireless communication under turbulence," *Photonics Res.*, vol. 3, no. 3, p. 48, Jun. 2015.

[24] M. Sharifzadeh and M. Ahmadirad, "Performance analysis of underwater wireless optical communication systems over a wide range of optical turbulence," *Opt. Commun.*, vol. 427, no. June, pp. 609–616, 2018.

[25] J. Armstrong and B. J. C. Schmidt, "Comparison of asymmetrically clipped optical OFDM and DC-biased optical OFDM in AWGN," *IEEE Commun. Lett.*, vol. 12, no. 5, pp. 343–345, 2008.

[26] S. D. Dissanayake and J. Armstrong, "Comparison of ACO-OFDM, DCO-OFDM and ADO-OFDM in IM/DD systems," *J. Light. Technol.*, vol. 31, no. 7, pp. 1063–1072, 2013.

[27] J. Lian, Y. Gao, P. Wu, and D. Lian, "Orthogonal frequency division multiplexing techniques comparison for underwater optical wireless communication systems," *Sensors (Switzerland)*, vol. 19, no. 1, pp. 1–19, 2019.

[28] D. Tsonev *et al.*, "A 3-Gb/s single-LED OFDM-based wireless VLC link using a Gallium Nitride μLED," *IEEE Photonics Technol. Lett.*, vol. 26, no. 7, pp. 637–640, 2014.

[29] S. Dimitrov, S. Sinanovic, and H. Haas, "Clipping noise in OFDM-based optical wireless communication systems," *IEEE Trans. Commun.*, vol. 60, no. 4, pp. 1072–1081, 2012.

[30] L. Chen, B. Krongold, and J. Evans, "Performance analysis for optical OFDM transmission in short-range IM/DD systems," *J. Light. Technol.*, vol. 30, no. 7, pp. 974–983, 2012.

[31] T. Fath and H. Haas, "Performance comparison of MIMO techniques for optical wireless communications in indoor environments," *IEEE Trans. Commun.*, vol. 61, no. 2, pp. 733–742, 2013.

[32] M. V. Jamali *et al.*, "Statistical studies of fading in underwater wireless optical channels in the presence of air bubble, temperature, and salinity random variations," *IEEE Trans. Commun.*, vol. 66, no. 10, pp. 4706–4723, 2018.

[33] S. M. Navidpour, M. Uysal, and M. Kavehrad, "BER performance of free-space optical transmission with spatial diversity," *IEEE Trans. Commun.*, vol. 6, no. 8, pp. 2813–2819, 2007.